Research article

Journal of RAMAN SPECTROSCOPY

Received: 13 February 2012 Revised: 10 July 2012 Accepted: 30 August 2012 Published online in Wiley Online Library

(wileyonlinelibrary.com) DOI 10.1002/jrs.4195

Determination of one-dimensional spherically aberrated point spread function in depth profiling by confocal Raman microscopy

María de la Paz Miguel and J. Pablo Tomba*

We present a simple experiment that allows the complete and direct characterization of the point spread function (PSF) in refraction-aberrated depth profiling experiments with confocal Raman microscopy. We used a wedge-shaped solid polymer film to induce refraction aberrations on the response of an infinitesimally thin Raman scatterer, represented by a polished silicon wafer. The system, with the film pasted on top of the Si wafer, was probed by a depth slicing technique under a dry-optics configuration. Post-acquisition processing of the Si and polymer intensity maps allowed the reconstruction of the axial PSF spatially resolved each 1 μm or less in the z-axis and for virtually continuous values of focusing depth. In agreement with theory, we found that PSF broadens asymmetrically with focusing depth, with a marked shift in the focus point. From the shape of PSF, we obtained values of depth resolution within the film that confirm that axial discrimination is not drastically deteriorated, as suggested by previous works, and that confocal aperture effectively reduces the collection volume even under severe refraction interference. Copyright © 2012 John Wiley & Sons, Ltd.

Keywords: confocal Raman microscopy; depth profiling; point spread function; refraction

Introduction

Confocal Raman microscopy is a remarkably versatile experimental tool for the physicochemical characterization of samples, with some unique characteristics. As in many other confocal techniques, it is possible, for instance, to gather spectroscopic information from within transparent materials without the need of physically sectioning the specimen. That probing mode, referred to as *optical sectioning*, can be applied to examine several families of transparent materials such as polymers and glasses, biological systems, coatings, fibers, cultural heritage, medicinal products, among others.

Many modern confocal microscopy techniques including Raman rely on the knowledge of the axial point spread function (PSF). This is a crucial determination not only to characterize depth resolution and overall instrumental conditions but also for other important reason. Since the response of an arbitrary sample feature is a convolution of the feature with the PSF, the knowledge of PSF would allow, in turn, the reconstruction of sample details with a higher level of precision by *deconvolution*. This is a rather well-developed strategy in fluorescence microscopy giving rise to a field known as *deconvolution microscopy*.[1] This kind of correction can be applied by numerical post-processing of the as-measured data, as a way of improving signal or image quality, where the success of this strategy relies on a rugged and precise scheme of characterization/prediction of PSF.[1,2] This concept can also be extended to Raman microscopy and has started to be explored in several recent publications.[3,4]

In theory, the axial PSF of a confocal microscope is limited by diffraction, with widths that depend on laser wavelength and on the inverse square of the numerical of the microscope objective employed.[5] In practice, the architecture of the confocal system, optical non-idealities and laser refraction due to the mismatch of refractive index along the laser pathway, i.e. between the objective nose and the focusing point within the sample, may also affect the widths and shape of PSF.[6,7] In Raman microscopy, a very flexible configuration, preferred for many users and virtually compatible with all the samples, is that based on the employment of standard metallurgical objectives (dry optics) where the laser beam is focused in the sample through air. It is well known that in that configuration, the air/sample mismatch in refractive index introduces substantial laser refraction, which broadens PSF with increasing focusing depth, well beyond the diffraction limit, and causes a focal shift or artificial compression of the objects on the depth scale. Despite the above mentioned problems, that configuration is many times preferred over the use of the more precise immersion optics, designed to minimize refraction aberrations through the use of a coupling fluid that fills the space between objective and sample. Generally, immersion objectives are more expensive than dry counterparts, besides the fact that there is a risk of sample damage by contact with the coupling fluid and that the presence of overlapping fluid peaks may complicate data analysis. In addition, recent work has shown that corrections by numerical post-processing of experiments acquired with dry optics may help in improving data quality at the same level than that obtained with immersion optics.[8]

The characterization of refraction-aberrated PSF in Raman microscopy has been approached theoretically by several models that describe the problem with different levels of rigor and sophistication. We may find from simple treatments based on

* *Correspondence to: Juan Pablo Tomba, Institute of Materials Science and Technology (INTEMA), National Research Council (CONICET), University of Mar del Plata, Juan B. Justo 4302, (7600) Mar del Plata, Argentina. E-mail: jptomba@fi.mdp.edu.ar*

Institute of Materials Science and Technology (INTEMA), National Research Council (CONICET), University of Mar del Plata, Juan B. Justo 4302, 7600 Mar del Plata, Argentina

geometric optics developed by Everall and Bachelder,[6,9] to more complex but rigorous description based on vectorial theory given by Sourisseau.[10] With any of these treatments, it is possible to predict PSF as a function of focusing depth, sample refractive index and details of the optical configuration such as type of objective and size of the confocal aperture. These predictions have been *indirectly* tested by comparing convoluted responses with experimental data, typically obtained from model samples with well-defined features. However, there is a lack of experiments aimed at *directly* measuring refraction-aberrated PSF in order to proceed to a straight verification of model predictions.

We believe that an experimental approach to PSF characterization is very useful not only to validate the above mentioned models but also to establish a solid baseline for deconvolution microscopy, particularly when measurements are dominated by refraction aberrations. This work describes how to carry out this task. The experimental setup was built by burying a silicon wafer under a polymeric substrate with variable thickness. Via optical sectioning of the specimen in the x-z plane, a methodology known as *depth slicing*, we were able to obtain, for the first time, a precise characterization of the shape of PSF as a function of the focusing depth and relevant conditions such as laser wavelength, confocality degree and sample refractive index.

Design of the experiment

This section describes the experimental assembly and the general strategy followed to obtain well-characterized PSF data from a depth slicing experiment. In all the cases, we assume a dry-optics configuration where samples are scanned through air. A classical test to determine the axial resolution of a confocal microscope consist in the scanning of a thin planar object along the optical axis, where depth resolution is defined as full width at half maximum (FWHM) of the response curve.[11] In Raman microscopy, a mirror-polished silicon wafer is commonly used with this purpose. As the laser beam does not penetrate into Si appreciably, typically less than 800 nm for a 514 nm laser wavelength, the polished surface essentially behaves as a layer of infinitesimal thickness thus providing a punctual response.[12] The penetration of that laser in germanium is even lower (~ 20 nm),[12] but this kind of sample is hardly available in a standard laboratory, despite the fact that Ge is a weaker scatterer than Si. Typically, the Si wafer is scanned in z direction, see Fig. 1(a), and the intensity of the 521 cm^{-1} Raman band plotted as a function of the microscope stage position. Thus, the obtained bell-shaped response represents the PSF in the absence of laser refraction and is usually reported as *nominal* depth resolution.[6] That response is also referred to as *diffraction-limited* depth resolution, although it may also reflect non-idealities of the optical system.

The situation changes when the Si wafer is profiled through a medium with refractive index about 1.5, for instance, a polymeric transparent film of known thickness, see Fig. 1(b). When the laser is focused at a certain distance below the surface of the polymer film, it deviates at the film entrance due to refraction thus shifting (and broadening) the original laser spot with focusing depth. For that reason, we introduce the Δ spatial domain; while z describes the true coordinate where the laser is actually directed, Δ measures the nominal focusing depth as read from the microscope stage scale. Both z and Δ have their origin at the sample surface.[6,7] Usually, PSF in refraction-aberrated experiments is defined in the z domain for a given value of Δ. In turn, the experiment described in Fig. 1(b) provides the response of a Si surface placed at a fixed value below the surface of the polymeric film, that is, we are basically sensing the response of the surface plane placed at a constant z value, determined by the film thickness. When profiling the system from the surface of the polymer film, we vary the values of Δ. Thus, the silicon profile yielded by this experiment can be seen as values of PSF corresponding to a family of Δ for a constant z, known in this case from the thickness of the polymer film if we assume perfect contact between Si and film surfaces.

The earlier experiment led us to think that depth profiling of Si wafers beneath a series of films with several thicknesses could

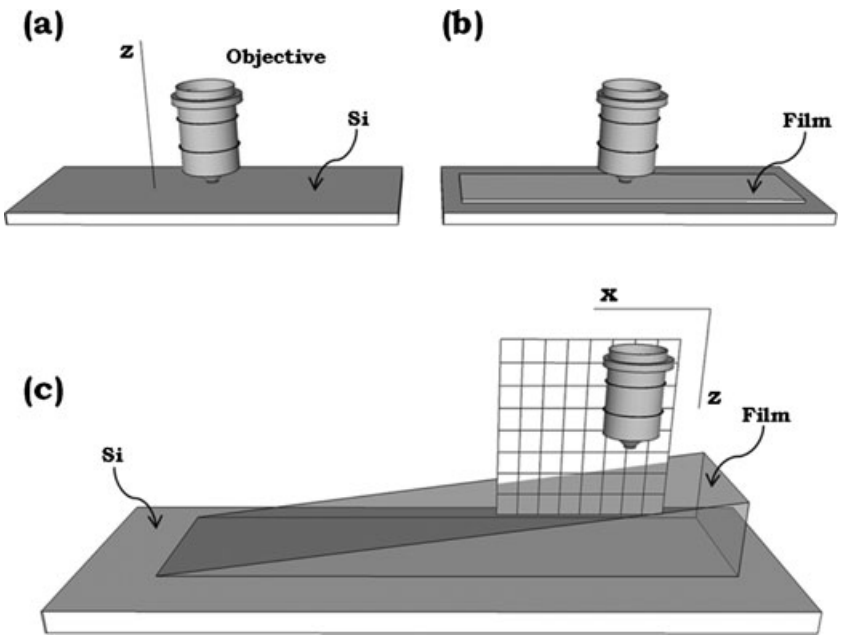

Figure 1. (a) Depth profiling of a bare Si wafer; (b) depth profiling of a Si wafer beneath a film of constant thickness; (c) depth slicing of a Si wafer beneath a wedged-shape film.

Journal of RAMAN SPECTROSCOPY

provide a set of values of Si responses for several Δ and as many z values as film thicknesses we probe, which would eventually yield a complete characterization of PSF. We have taken that concept but using a different strategy: instead of using multiple films, we propose the use of a single sample with variable thickness as shown in Fig. 1(c). For instance, a wedged-shape film fixed on the surface of a silicon wafer pasted on a slide would allow us to access to a wide and continuous range of film thicknesses (or z values), for several values of Δ. The experiment can be carried out in a single shot by using a depth slicing strategy, which basically consists in repeating several depth profiling measurements at different positions along the film.

In order to generate PSF in the more convenient fashion, i.e. a curves of depth response in the z scale for fixed values of Δ, we need to carefully consider a proper data processing, whose concept is described in Fig. 2. It is shown the basic set-up consisting in the polymeric film with variable thickness on top of the Si wafer along with a family of typical bell-shaped PSF expected for a specific value of the focusing depth, Δ_1. Several analysis lines placed at x_i positions along the film outer surface have also been included. Notice that the maximum of each PSF has been drawn shifted at larger depths with respect to Δ_1, to properly describe the effect of laser refraction. As the Si wafer essentially provides a punctual response, only the green dots of the PSF can be detected by tracking the Si Raman response. For instance, at Δ_1, we should not detect response from Si at positions to the right of x_2, such as x_1. The Si signal starts to be detected at x_2, see the green dot. The successive analysis at positions located from x_2 to x_5 yield Si intensities associated to other points of PSF as indicated with the green dots. Observe that there is a z_i value associated to each position x_i, which is given by the real thickness of the wedge at that position. Positions to the left of x_5 should not yield Si response at Δ_1, as PSF is completely below the surface of the Si wafer, and we assume that only the wafer surface yields Raman scattering.

In summary, obtaining PSF from this experiment requires: (1) the knowledge of the thickness of the wedge z_i for each x_i position, where z_i values are obtained from the profile of the polymer signal, see below; (2) Si intensity depth profiles for each x_i position. With these data, it is possible to build curves of the silicon intensity as a function of z for selected parametric values of Δ. More details about data processing will be given in the forthcoming sections.

Experimental

Raman spectra were recorded with a Renishaw in Via Reflex spectrometer system equipped with charge-coupled device (CCD) detector of 1040 × 256 pixels and coupled to a Leica microscope with a computer-controlled x-y-z stage. An Ar laser line (514 nm, 50 mW) was used as excitation source in combination with a grating of 2400 grooves/mm. The laser power was kept below 10% to avoid sample damaging while keeping good spectra quality. A Leica metallurgical objective 100× (0.9 NA) was used in the excitation and collection path. Confocality for light collection was achieved by tuning the pixel binning of the spatial dimension of the CCD and the aperture of the spectrograph entrance slit. Two predetermined confocality configurations, high (3 pixels of the CCD, 20 μm slit opening) and regular (6 pixels of the CCD, 65 μm slit opening) were used; these configurations are analogous to small and large confocal apertures in pinhole-based instruments.

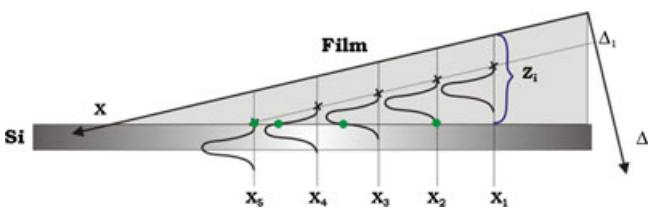

Figure 2. Scheme of experimental setup. The bell-shaped curves represent PSF for a given value of focusing depth, Δ_1, as measured from the film surface, for several positions throughout the film surface (x_i). Both z and Δ scales have their zeroes at the film surface. The green dots represent the detected values of PSF from the response of the Si wafer.

Thin wedged-shape films were fabricated with polystyrene (refractive index, $n = 1.59$), a solid material at room temperature, chosen for its high grade of transparency. The virgin sample was placed between a pair of glass slides, with spacers to control sample thickness, and melted in a carver press at 150 °C. Specimens were shaped to be mounted on microscope slides. Thicknesses were designed to be compatible with the microscope objective working distance (270 μm) and with the effect of compression of the axial scale by refraction. Typical specimen slopes were about 1 μm in z each 50–100 μm in x. The horizontal wedge surface was attached to a polished-to-mirror silicon wafer pasted on a slide. To achieve good optical contact between the solid wedge and Si, a drop of ethylene glycol was added between them.

The whole specimens were subjected to x-z depth slicing experiments, as depicted in Fig. 1(c). Once the film surface was in-focus, a line along x was drawn on the software video image to define the grid of analysis. Step sizes in x direction were typically 50–100 μm, to cover analysis length of about 3000–4000 μm in the x scale. Step sizes in z direction were set to 1–2 μm. Each point spectrum was taken with an exposure time of 1 s and two accumulations. A typical experiment involves about 2000–4000 point spectra, which takes 1–3 h of analysis. That time can be quite reduced using fast mapping techniques or a grosser grid, although none of these strategies were employed here. Invariance of instrumental conditions was verified at the beginning and end of each experiment by running an internal Si sample.

Home-made software was developed in FORTRAN to facilitate data handling and PSF construction. The depth slicing experiment generates a set of data that basically consist in one spectrum for each set of x-z positions. Data processing begins with the creation of a map of components from the depth slicing spectra, carried out with the instrumental software.[13] The analysis generates two files, one for each component, PS and Si, with a common three columns structure: the first column corresponds to the instrumental axial scale (or microscope stage axial position), the second one to the position on the x scale and the third one to the component intensity for those two spatial coordinates. A first FORTRAN unit reorganizes the data in a new data matrix where the first column allocates values of the instrumental axial scale while the rest of the columns correspond to intensity values that share a common x position. In that way, plotting the first column of that matrix *versus* any of the other columns yields an intensity depth profile of either PS or Si for a given x_i position, of the type shown in Fig. 4, see below. In particular, the analysis of the PS profile allows the identification of the position of the PS surface on the axial scale, which gives access to z_i values, see discussions on Fig. 4 below for more details. Those z_i values, one for each column (or x_i positions), are stored in a separate file. A second FORTRAN unit generates PSF from the Si

data file, for a given value of Δ set by the user. The program seeks in each of the intensity columns for values placed at Δ units below the position of the PS surface (z_i), using the values of the first column as a reference. Linear interpolation is applied when the data lies in between those recorded. Then, the value of Si intensity found is linked to the value of z_i corresponding to that column, defining a series of intensity-*versus*-z pairs that characterize PSF.

Results and discussion

Figure 3 shows the typical Raman map of components of the composite PS–Si system as revealed by the x-z depth slicing technique. Data were obtained with a 0.9 NA dry objective in the high confocality (HC) mode, a setup that usually yields the best attainable nominal depth resolution. The image was constructed by component analysis on the base of pure Si and PS Raman spectra,[13] where variations in colour and intensity are related to their respective localization. The thin green band corresponds to the surface of the Si wafer, while the broader and variable in thickness red one corresponds to the PS wedge made film. The dark zones in the image are most likely due to the presence of small voids produced during PS sample fabrication.

In the image, we refer z* as the instrumental axial scale. For the sake of convenience, see below, we set z* at 0 on the *real* position of the Si surface, which also corresponds to the Si/PS film interface if we assume good contact between layers. With this choice, z* has positive values above the Si wafer or within the PS film as observed in the image. Due to refraction aberrations, the position of the Si surface appears sloped and artificially closer to the outer face of the PS layer: on the left end, it appears positioned at 40 μm while on the right at 75 μm on the z* scale, despite the fact that we previously zeroed z* at the Si surface. The thickness of the PS layer is also distorted by the same effect. On the other hand, the outer surface of the PS wedge, exposed to air, appears in the image at their correct values as they are not distorted by refraction. In fact, the real thickness of the PS wedge can be readily inferred for any point in x from the z* value on the PS surface, as we zeroed the instrument at the silicon/film interface. For instance, Fig. 2 shows that the real thickness of the PS layer varies from about 170 μm at x = 0 to 100 μm at x = 4000 μm. As we will see, the knowledge of the correct positioning of the PS outer surface is vital for PSF construction.

The map of components is processed to obtain the PS and Si intensity profiles as a function of z* for several points on the x scale, according to the selected measuring range. Typical data are shown in Fig. 4, for an arbitrary fixed x_j position. It can be seen that the PS intensity grows suddenly at the air/PS interface (z* ~ 112 μm), up to reach a maximum, followed by a smooth decay inside the polymer. Eventually, the Si/PS interface is reached and the PS signal drops off to values close to zero. We also observe that we detected PS signal above the PS film (z* > 112 μm), in the form of a tail preceding the PS maximum, which is a manifestation of the confocal response at the so-called diffraction limit, as laser refraction at the PS/air interface is virtually suppressed. On the other hand, the silicon profile appears as a broad peak distorted by all the combined optical distortions. Once again, notice that the PS–Si interface appears artificially closer to the outer surface of the polymer coating due to the spatial compression caused by refraction.

From the results shown in Fig. 4, we readily obtain: (1) the position of the outer PS layer, from the derivative of the PS intensity profile, which equals to the true position of the Si surface and defines the value of z_i (112 μm in the example of Fig. 4); (2) the corresponding Si intensity for a given Δ_1 value (I_{Δ_1,z_i}), where Δ_1 is read from the same z* scale but zeroed at the outer PS surface, the norm in depth profiling experiments. Processing these data for the complete specimen, as explained in the experimental section, allows the construction of PSF plots as a function of z for selected values of Δ.

Figure 5(a) shows a family of PSF plots obtained with the procedure above described, from data acquired in the following conditions: 514 nm laser wavelength focused through a medium with $n = 1.59$ (PS), via a dry 0.9 NA objective in HC. The data shown correspond to several values of Δ, arbitrary spaced each 5 μm, where the range covered, i.e. 20–100 μm, is that usually probed with high performance metallurgical objectives. On the other hand, the interval in the z scale is basically determined by the slope of the wedge and the x-step size chosen in the depth slicing experiment. We optimized those parameters in order to obtain data with z intervals in the order 1 μm (or even lower), which, as we see, are enough refined to properly resolve the refraction-aberrated PSF. Remarkably, the data shown

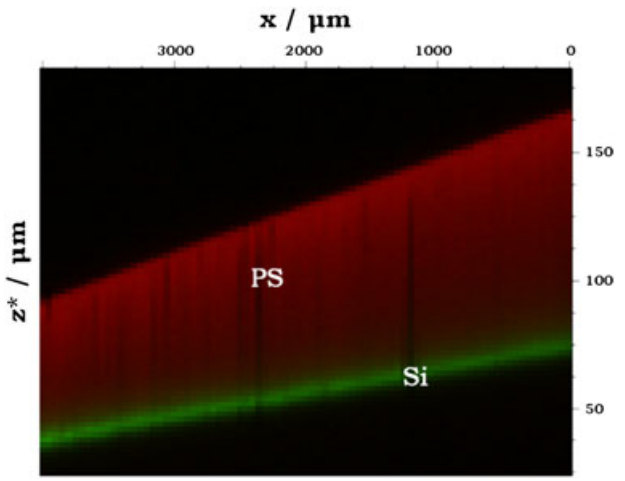

Figure 3. Raman image obtained from the depth slicing experiment. The z* scale was zeroed at the real position of the Si/PS interface.

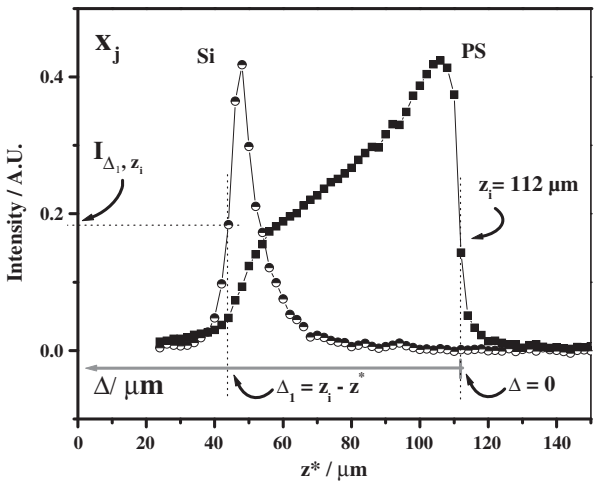

Figure 4. A typical Si and PS film depth profiles, obtained at a given x_j position of the PS surface. Relevant parameters needed for PSF construction, z_i, Δ_1 and $I(\Delta_1,z_i)$ are indicated.

Journal of RAMAN SPECTROSCOPY

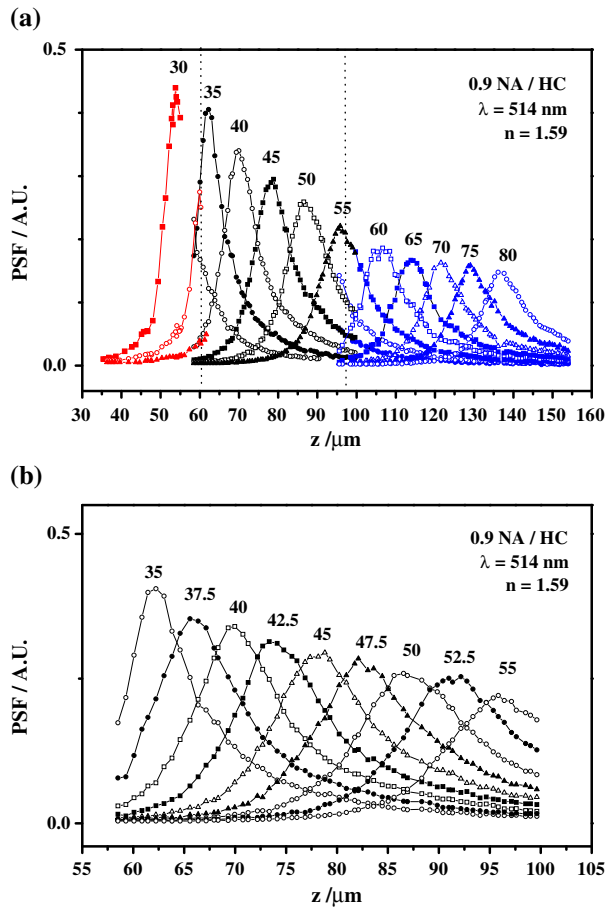

Figure 5. As obtained PSF family from the depth slicing experiment for the instrumental conditions indicated. Numbers on top of each curve indicate Δ values in μm. Intervals in Δ were set to: (a) 5 μm; (b) 2.5 μm.

correspond to an assembly of three independent experiments, carried out over three entirely different PS samples and run over different days; each run has been represented with a different colour. The superposition between the three experimental windows is a good example of experiment consistency, although the whole set of data could have been readily generated using a single sample and in one shot. Figure 5(b) shows a finer view of a family of PSF in the range of Δ values 35–55 μm, with a finer spacing (2.5 μm), to demonstrate that the experiment allows a virtually continuous and well-detailed monitoring of PSF evolution.

Figure 6 shows selected plots of PSF curves in four panels, to emphasize some relevant details of the data. Figure 6(a) shows the PSF at Δ = 40 μm (symbol) compared with the response obtained from the bare Si wafer (solid line), typically informed as nominal (diffraction-limited) depth resolution, for the 0.9 NA/HC combination. It can be observed that the aberrated-PSF changes appreciably in shape with depth turning broader and asymmetric as predicted by theory.[9,10,14] The asymmetry of PSF can be explained in terms of the non-invariant distortion caused by laser refraction which continuously broadens both incident and collected responses, with the increase in focusing depth.[6,9] Depth resolution, as estimated from the FWHM criterion, worsens from a value of 2.3 μm (bare Si) to about 10 μm at 40 μm depth, indicating that refraction becomes the dominant distorting effect at large depths. The response is also shifted at larger depths with a maximum at 70 μm for a nominal focusing depth of 40 μm. The focus displacement corresponds in this case to a factor of 1.75, which compares very well with data previously published on artificial compression of sharp interfaces measured in similar instrumental conditions and with rigorous theoretical simulations of refraction effects on PSF.[10,15] All these features, characteristic of depth profiling with dry objectives, are clearly captured by the experiment and first seen in terms of directly measured PSF.

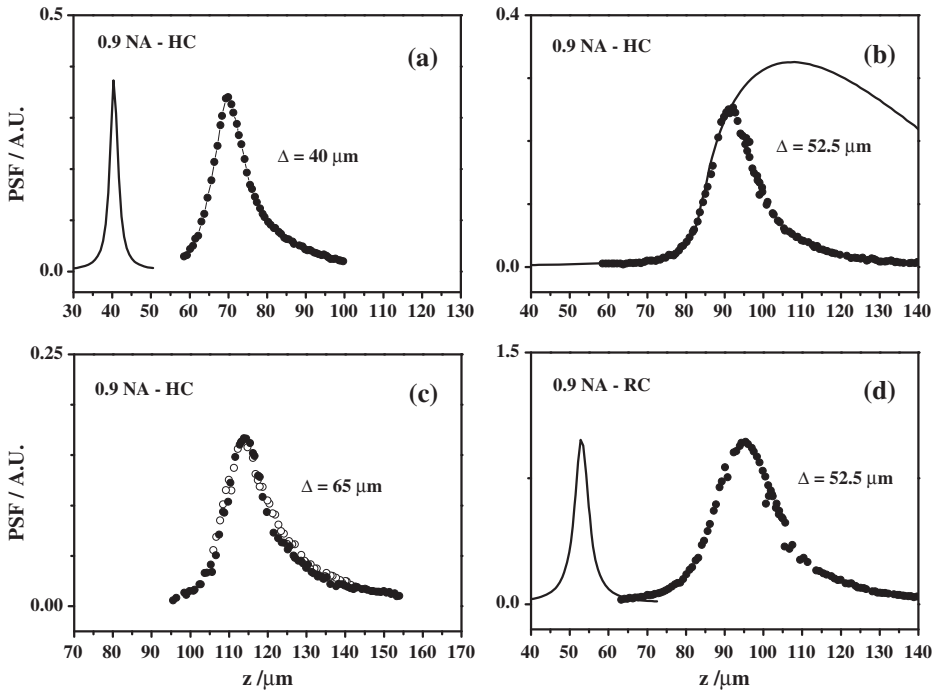

Figure 6. Axial PSFs for a dry objective 0.9 NA/high and different values of Δ, as indicated. HC: high confocality; RC: regular confocality. The laser was in all the cases 514 nm and the sample refractive index, 1.59.

Figure 6(b) shows the as measured PSF corresponding to $\Delta = 52.5\,\mu m$, along with a prediction based on the model of Everall, in solid line.[6,7] The above-mentioned model describes the effect of laser refraction on an originally point-focused laser spot, but without considering neither diffraction nor the effect of the confocal aperture in the collection path. The model has been properly modified to account for the original axial dimensions of the laser beam, which, as a consequence of diffraction, is not infinitesimally sized, but still without accounting for the confocal aperture.[14] We see that the depth responses measured and predicted are in excellent agreement, particularly in the range 80–95 μm, but that they depart markedly beyond 90 μm. The abrupt cut-off observed in the experimental data can be attributed to the confocal hole, which effectively blocks scattering arising from larger depths, as originally predicted by theoretical work of Batchelder.[9] We can directly see, for the first time, that the confocal aperture plays an important role in preserving depth resolution at reasonable values (~13 μm) even in experiments largely affected by laser refraction. This statement, first suggested by Sourisseau and coworkers, can be now certainly confirmed.[10,16] On the other hand, the shift in the focus point, inherent to experiments under mismatch in refractive index, cannot be avoided.

Figure 6(c) shows PSF obtained from two entirely different PS samples, as shown with open and filled circles, at still larger focusing depths (65 μm). Compared with the responses shown at 40 and 52.5 μm, PSF is somewhat broader (FWHM = 15 μm), with a focus shift by about the same factor. The superposition between PSF obtained from independent samples illustrates the very nice experiment reproducibility in terms of both sample preparation and instrumental stability.

Figure 6(d) shows the depth response obtained with a larger confocal aperture (regular confocality), at a focusing depth of 52.5 μm. As a reference, the response of the bare Si wafer in regular confocality has also been included (solid line). Although the overall PSF shape is preserved when compared with that generated in HC, the response shows a smothered shape, with slower decays below and above its peak. Because of the larger confocal aperture, the cut-off is shifted to somewhat larger depths, which also shifts the PSF maximum, now placed at $z = 95\,\mu m$. Depth resolution calculated from the FWHM criterion indicates that it worsens from 4.3 μm (bare Si) to about 19 μm (regular) at 52.5 μm depth. That value also worsens with respect to that found in HC (13 μm), but keeping the advantage of working with at least a threefold increase in collected Raman scattering due to the larger confocal aperture.

Conclusions

We have presented a rather simple strategy based on depth slicing of a model system which allowed, for the first time, the direct measurement of refraction-aberrated PSF in confocal Raman microscopy. Data were obtained with outstanding definition and in a suitable form to be compared with numerical models that predicts one PSF for each focusing depth. In agreement with theory, the non-invariant behaviour of the axial PSF in confocal Raman microscopy was verified: the focus point shifts to larger depths with a simultaneous asymmetric broadening. For typical values of focusing depth, depth resolution worsens by almost one order of magnitude compared with nominal values determined; however, these values are rather smaller than that suggested by preliminary theories that ignore the effect of the confocal aperture. Overall, the availability of well-characterized PSF experimental data is very helpful to enhance methodologies of data analysis and to provide a deeper understanding of the factors that control depth-profiling with Raman microscopes.

Acknowledgements

This work was supported by ANPCYT through PICT06-1359 and PICT10-284. We would like to thank Prof. José M. Carella for preparing the PS laminate sample.

References

[1] J. B. Sibarita, *Adv. Biochem. Engin./Biotechnol.* **2005**, *95*, 201.
[2] W. Wallace, L. H. Schaefer, J. R. Swedlow, *Biotechniques* **2001**, *31*, 1076.
[3] J. P. Tomba, M. P. Miguel, C. J. Perez, *J. Raman Spectrosc.* **2011**, *42*, 1330.
[4] A. Gallardo, S. Spells, R. Navarro, H. Reinecke, *J. Raman Spectrosc.* **2007**, *38*, 880.
[5] C. B. Juang, L. Finzi, C. J. Bustamante, *Rev. Sci. Instrum.* **1988**, *59*, 2399.
[6] N. Everall, *Appl. Spectrosc.*, **2000**, *54*, 773.
[7] N. Everall, *Appl. Spectrosc.*, **2000**, *54*, 1115.
[8] M. P. Miguel, J. P. Tomba. *Progr. Org. Coat.* **2012**, *74*, 43.
[9] K. J. Baldwin, D. N. Batchelder, *Appl. Spectrosc.* **2001**, *55*, 517.
[10] C. Sourisseau, P. Maraval, *Appl. Spectrosc.* **2003**, *57*, 1324.
[11] C. J. Grauw, M. W. Sijtsema, C. Otto, J. Greeve, *J. Microsc.* **1997**, *188*, 273.
[12] Horiba Scientific, Application Notes **2011**, RA39.
[13] J. P. Tomba, E. de la Puente, J. M. Pastor, *J. Polym. Sci., Part B: Polym. Phys.* **2000**, *38*, 1013.
[14] J. P. Tomba, L. Arzondo, J. M. Pastor, *Appl. Spectrosc.*, **2007**, *61*, 177.
[15] N. Everall, *Appl. Spectrosc.* **2009**, *63*, 245A.
[16] J. L. Brunel, J. C. Lassegues, C. Sourisseau, *J. Raman Spectrosc.* **2002**, *33*, 815.

Research article

Determination of one-dimensional spherically aberrated point spread function in depth profiling by confocal Raman microscopy

María de la Paz Miguel and J. Pablo Tomba

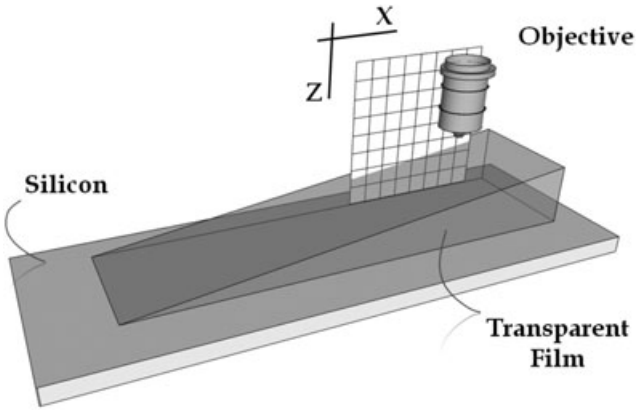

We present a simple experiment that allows full characterization of the point spread function (PSF) in refraction-aberrated depth profiling experiments with confocal Raman microscopy. We used a wedge-shaped solid polymer film to induce refraction aberrations on the response of an infinitesimally thin Raman scatterer (a silicon wafer). Via depth slicing of the specimen, we were able to directly characterize the shape of refraction-aberrated PSF as a function of the nominal focusing depth.